Science Advances

AAAS

advances.sciencemag.org/cgi/content/full/3/9/e1701301/DC1

Supplementary Materials for

Ultrahigh–current density anodes with interconnected Li metal reservoir through overlithiation of mesoporous AlF_3 framework

Hansen Wang, Dingchang Lin, Yayuan Liu, Yuzhang Li, Yi Cui

Published 8 September 2017, *Sci. Adv.* **3**, e1701301 (2017)
DOI: 10.1126/sciadv.1701301

This PDF file includes:

Supplementary Figures

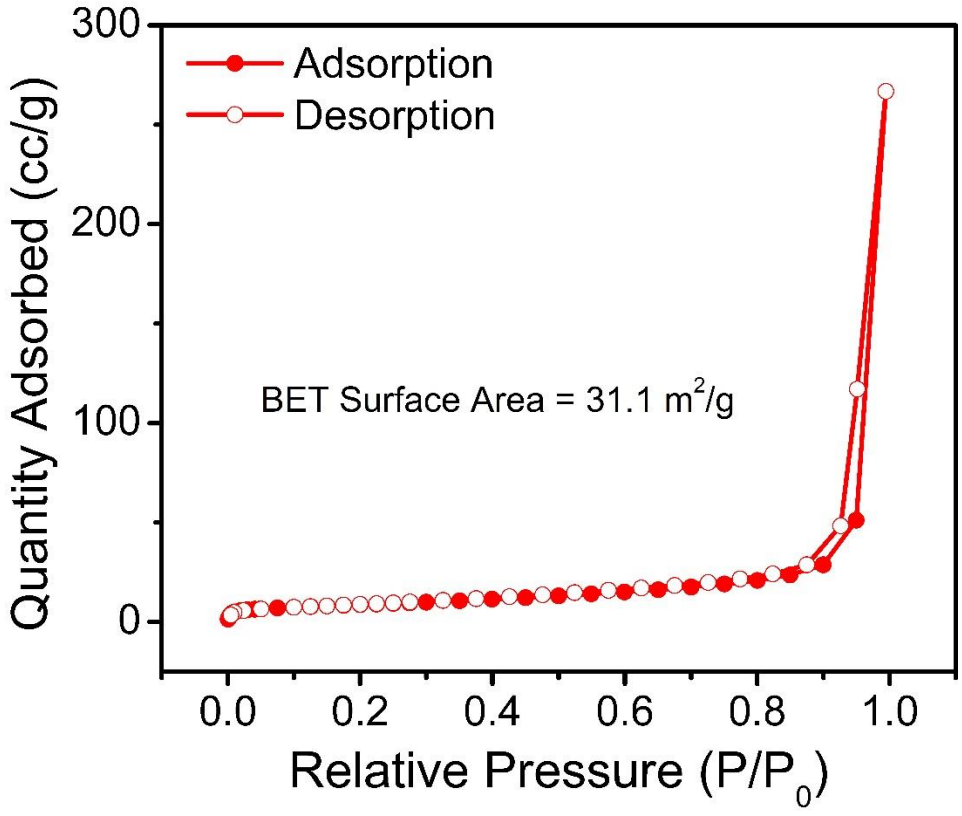

fig. S1. N_2 adsorption-desorption isotherm of AlF_3 powder.

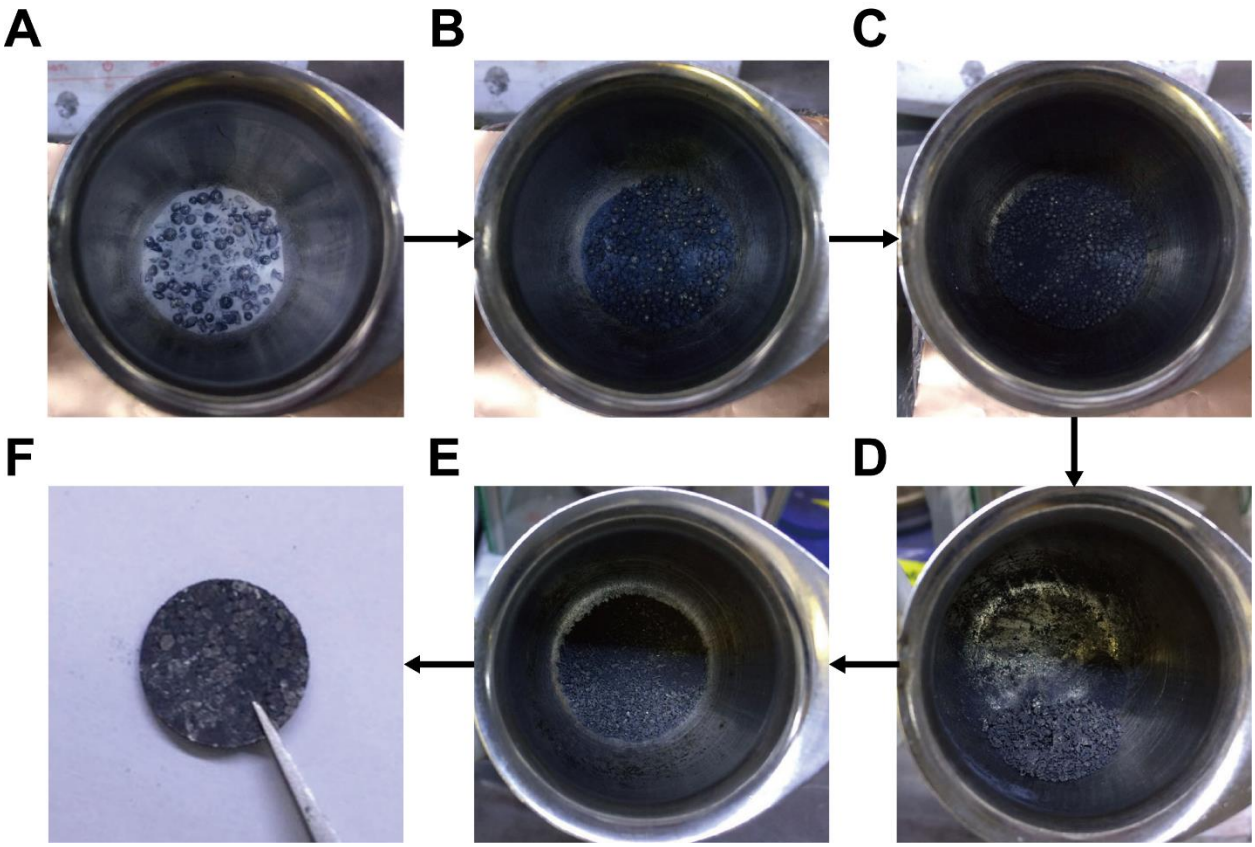

fig. S2. Fabrication of LAFN. (**A**) Digital photo of lithium metal being separated into small droplets among AlF_3 powder at the beginning of heating. (**B**) Digital photo of white powder turning into grey after stirring for 10 min. (**C**) Digital photo of powder turning into black and lithium droplets becoming smaller and infusing into mesoporous structure after stirring for 20 min. (**D**) Digital photo of LAFN pristine powder after cooling down. (**E**) Digital photo of LAFN powder after size selection. (**F**) Digital photo of LAFN electrode.

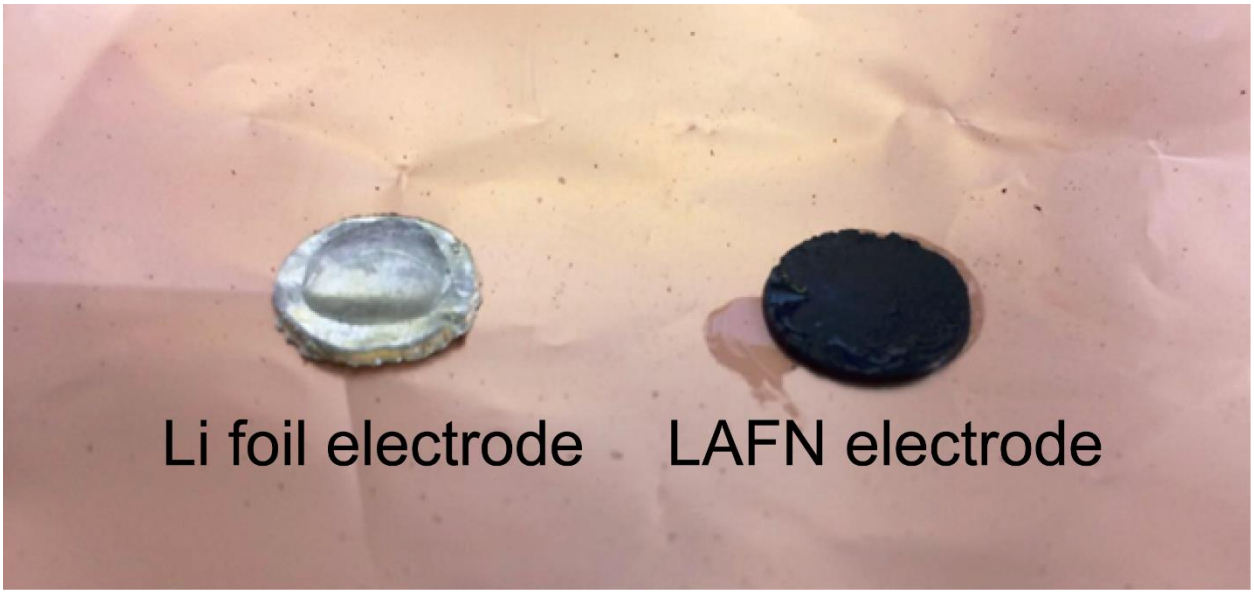

fig. S3. Digital photo of 20 µl of ethylene carbonate/diethyl carbonate electrolyte dropped onto Li foil and LAFN electrode. LAFN electrode takes up a large amount of electrolyte due to its pores between secondary particles.

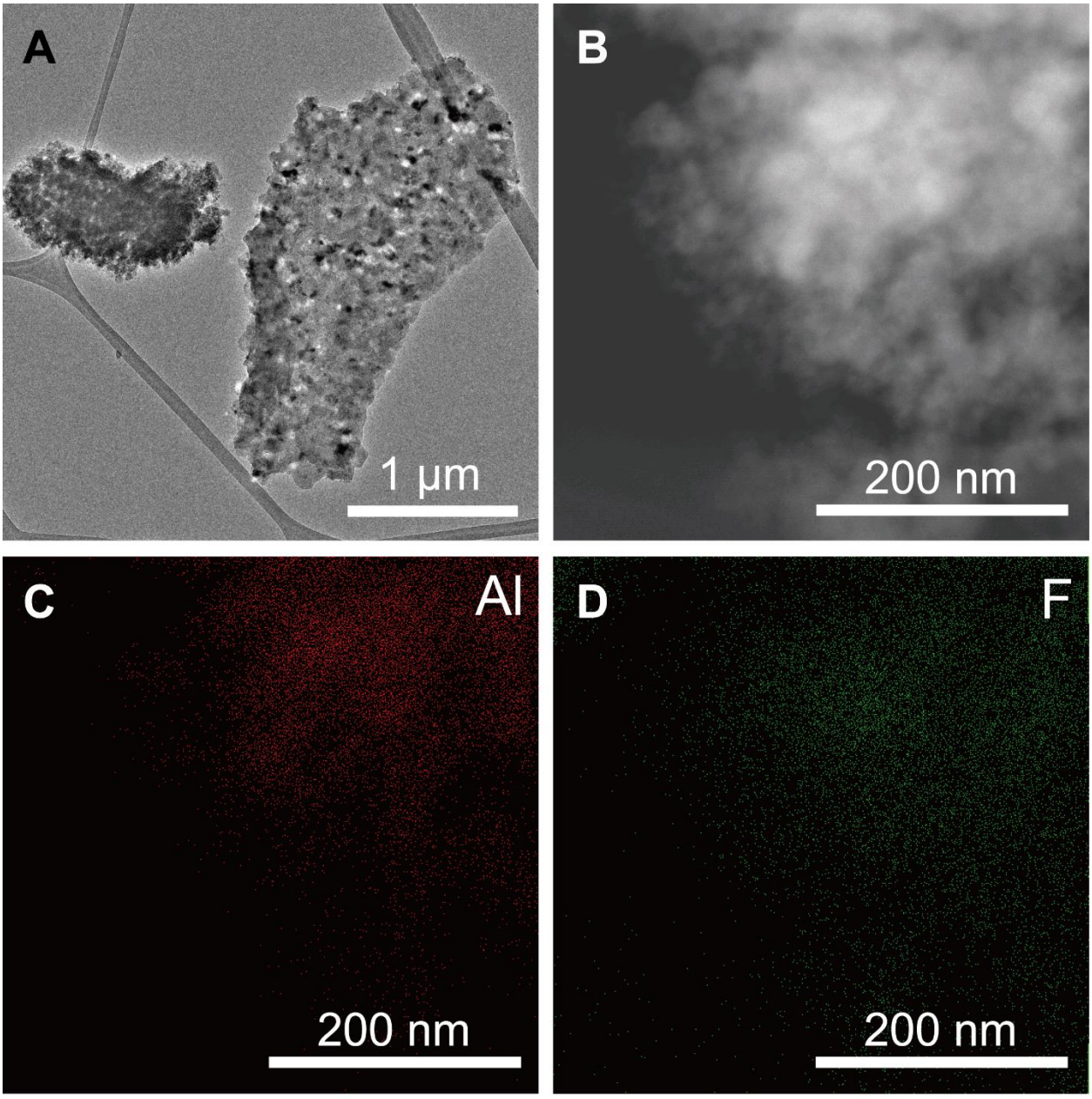

fig. S4. Transmission electron microscopy characterization of pristine LAFN. (**A**) Transmission electron microscope (TEM) image of LAFN secondary particles. (**B**) Scanning transmission electron microscope (STEM) image of part of a LAFN secondary particle. (**C** and **D**) Energy dispersive X-ray spectroscopy (EDX) mapping of Al (**C**) and F (**D**) in the region of **B**.

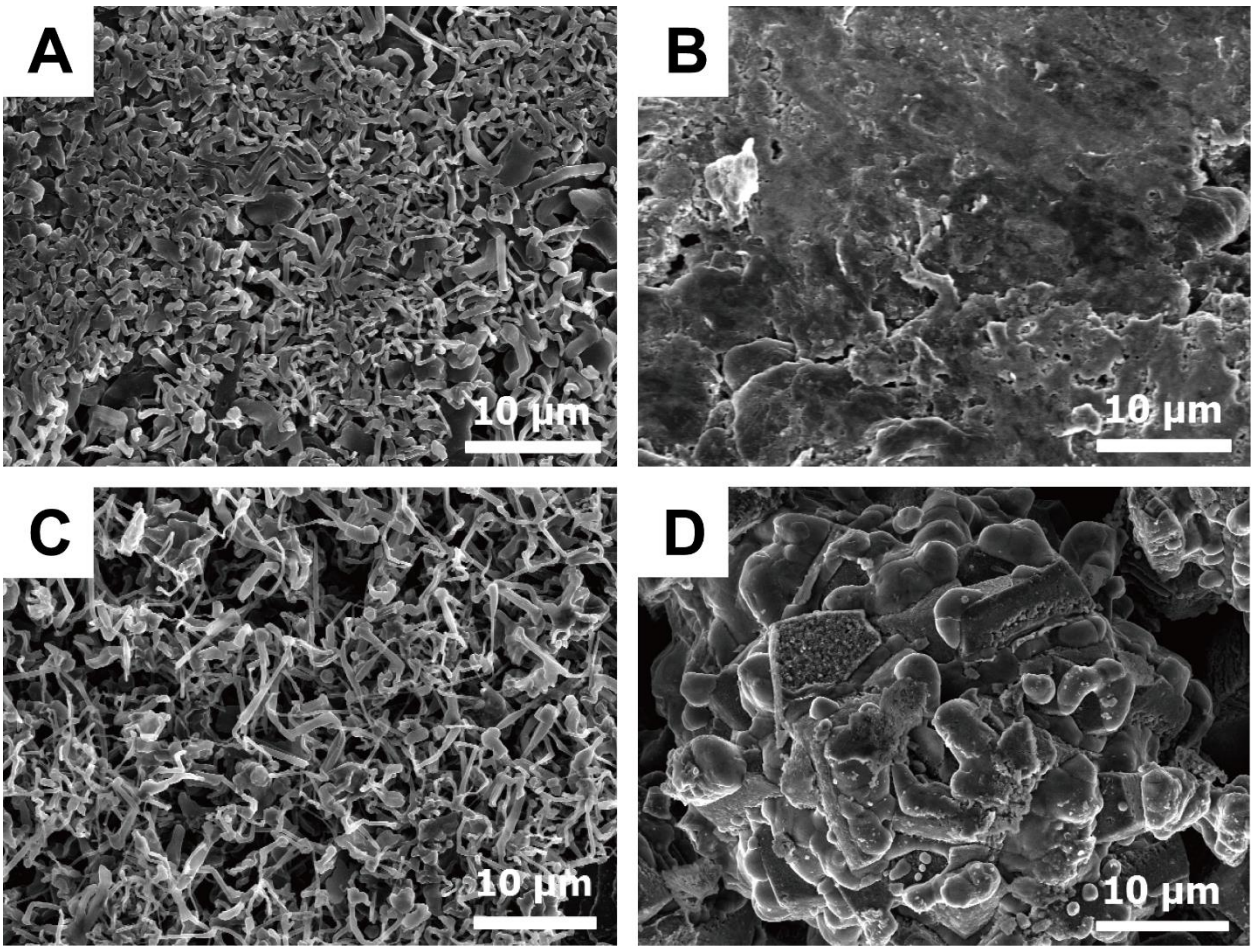

fig. S5. Morphology of LAFN after symmetric cell cycling. (**A** and **B**) Low magnification SEM images of Li foil surface (**A**) and LAFN (**B**) surface after 1 symmetric cell cycle under 1 mA cm^{-2}. (**C** and **D**) Low magnification SEM images of Li foil surface (**C**) and LAFN (**D**) surface after 1 symmetric cell cycle under 20 mA cm^{-2}. Areal capacity was fixed at 1 mAh cm^{-2}.

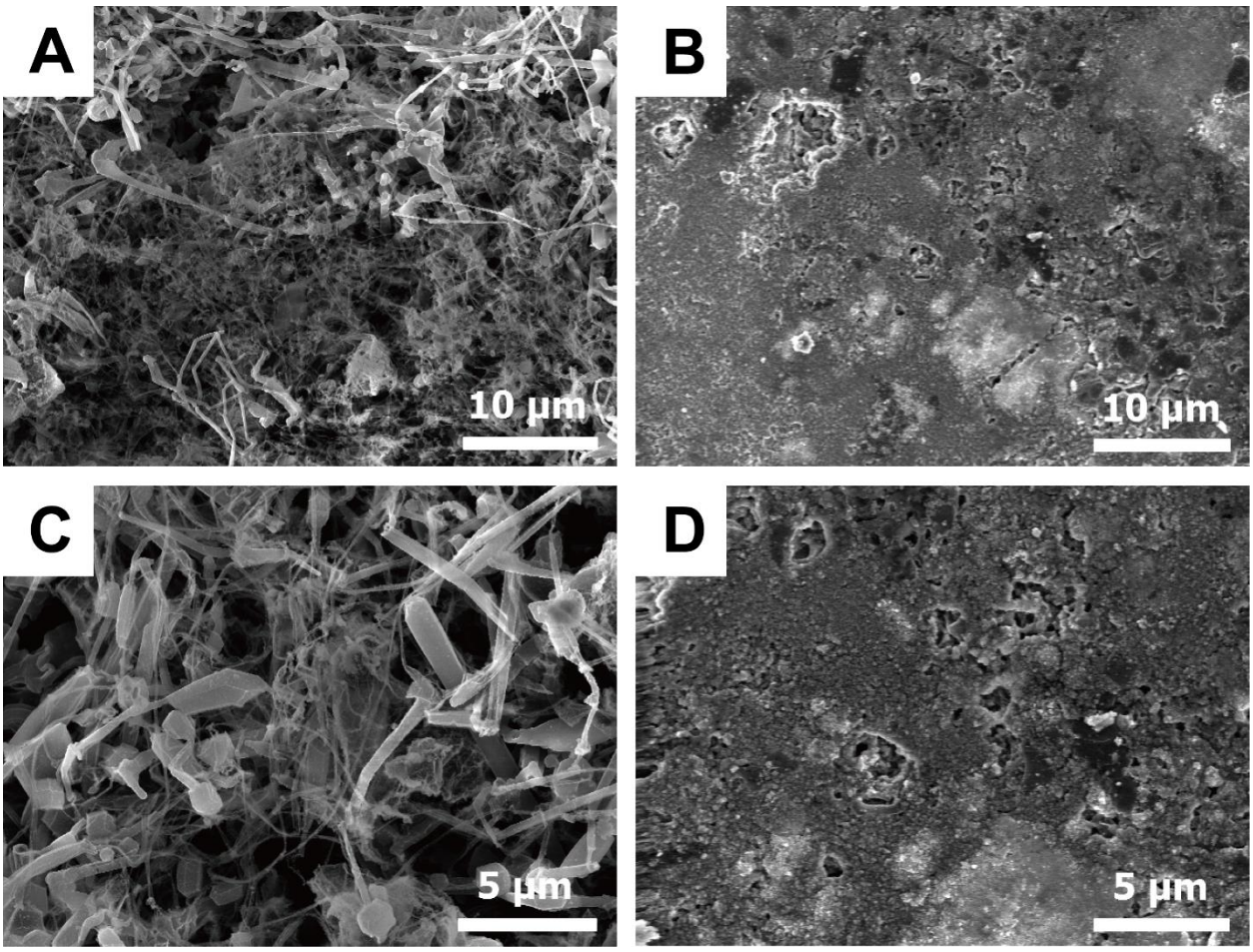

fig. S6. Morphology of LAFN after symmetric cell cycling. (**A-D**) Low magnification SEM images of Li foil surface (**A**) and LAFN (**B**) surface after 10 symmetric cell cycle under 1 mA cm^{-2}. High magnification SEM images of Li foil surface (**C**) and LAFN (**D**) surface after 10 symmetric cell cycle under 1 mA cm^{-2}. Areal capacity was fixed at 1 mAh cm^{-2}.

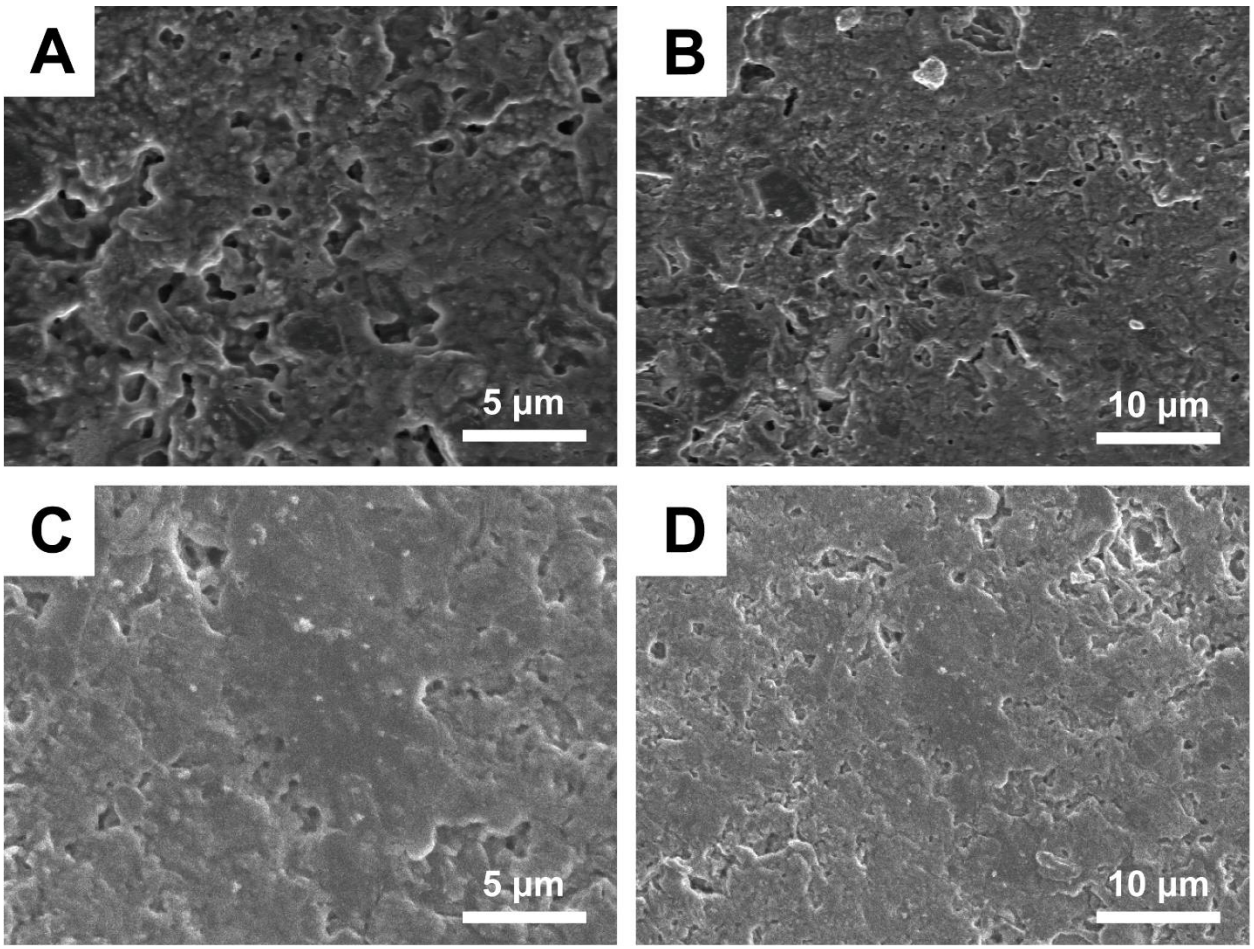

fig. S7. Morphology of LAFN after symmetric cell cycling. (**A** and **B**) SEM **i**mages of LAFN surface after 50 symmetric cell cycle under 1 mA cm^{-2}. (**C** and **D**) SEM images of LAFN surface after 100 symmetric cell cycle under 1 mA cm^{-2}. Areal capacity was fixed at 1 mAh cm^{-2}.

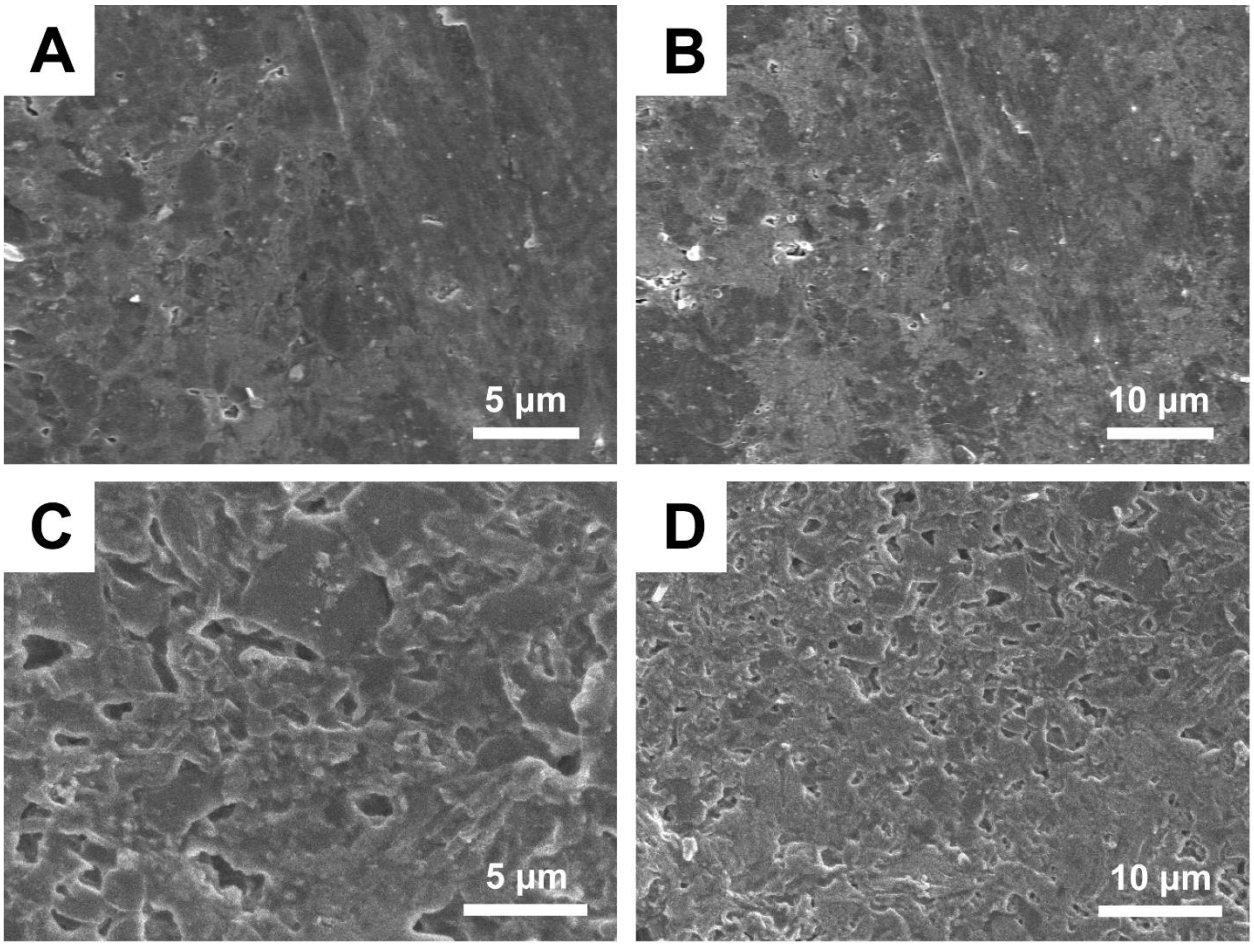

fig. S8. Morphology of LAFN after symmetric cell cycling. (**A** and **B**) SEM **i**mages of LAFN surface after 10 symmetric cell cycle under 1 mA cm^{-2}. (**C** and **D**) SEM images of LAFN surface after 30 symmetric cell cycle under 1 mA cm^{-2}. Areal capacity was fixed at 3 mAh cm^{-2}.

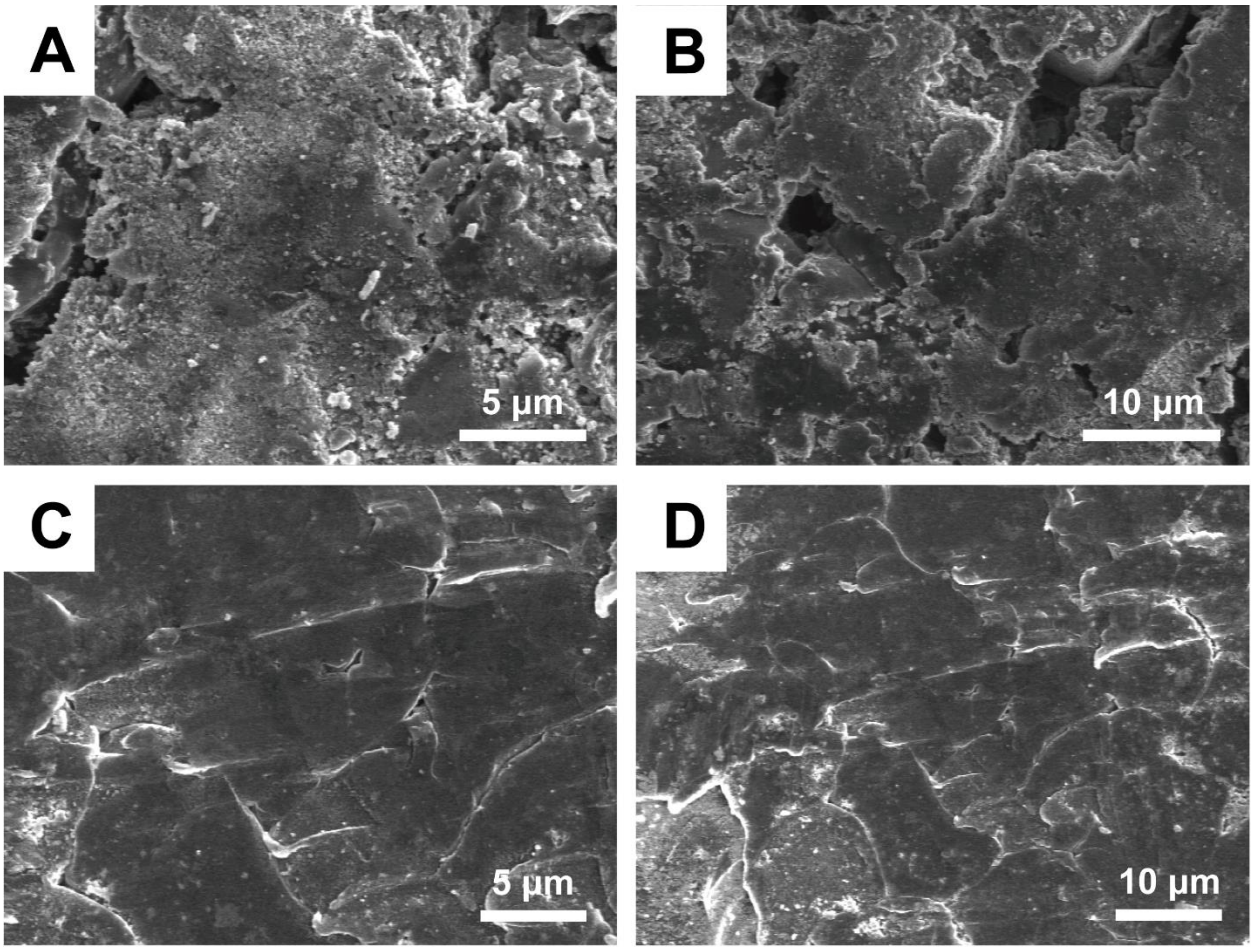

fig. S9. Morphology of LAFN after directly plating Li metal onto its surface. (**A** and **B**) SEM **i**mages of LAFN surface after plating 1 mAh cm^{-2} Li metal. (**C** and **D**) SEM **i**mages of LAFN surface after plating 5 mAh cm^{-2} Li metal.

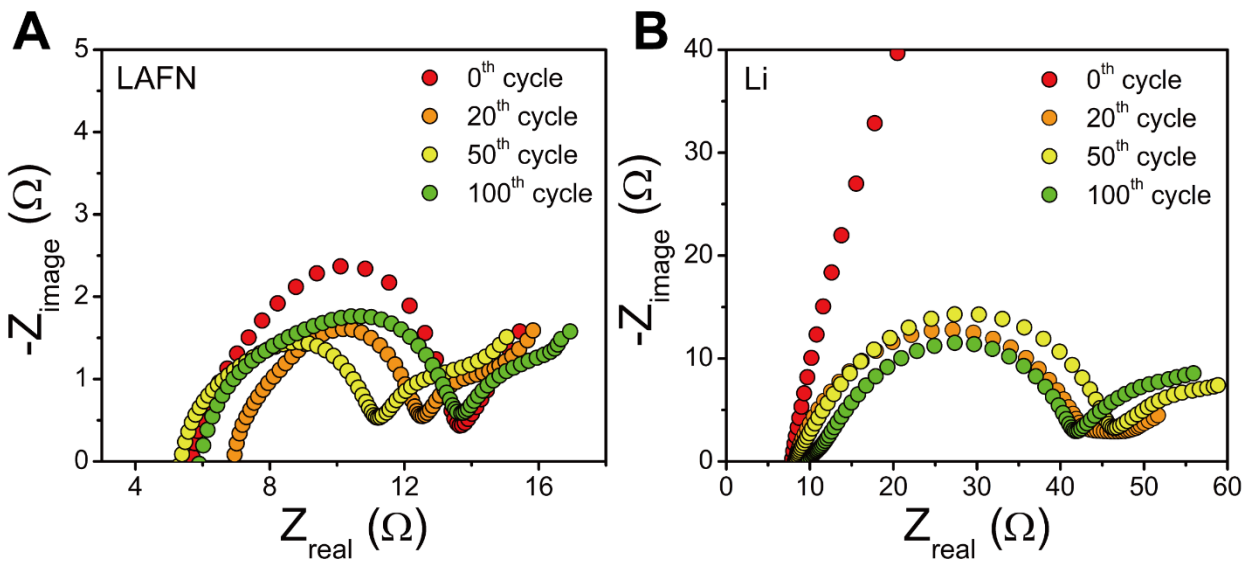

fig. S10. EIS performance of Li foil and LAFN symmetric cells after different cycles.

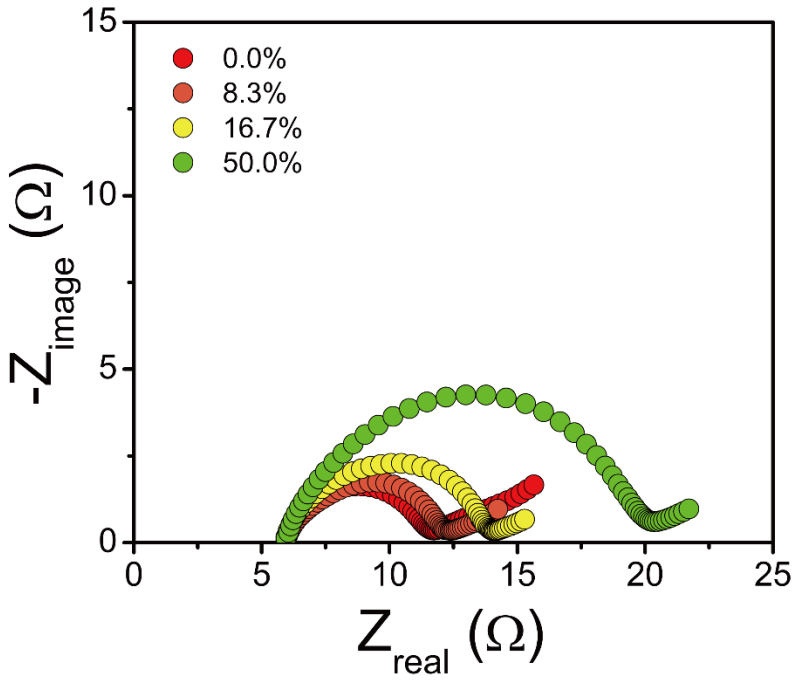

fig. S11. EIS performance of LAFN symmetric cells after stripping different percentages of capacity from one side to the other. Here the LAFN electrodes were made of 0.04 g of LAFN powder, offering a capacity ~ 60 mAh. And the percentage here shows how much capacity of Li metal were stripped from one side to the other.

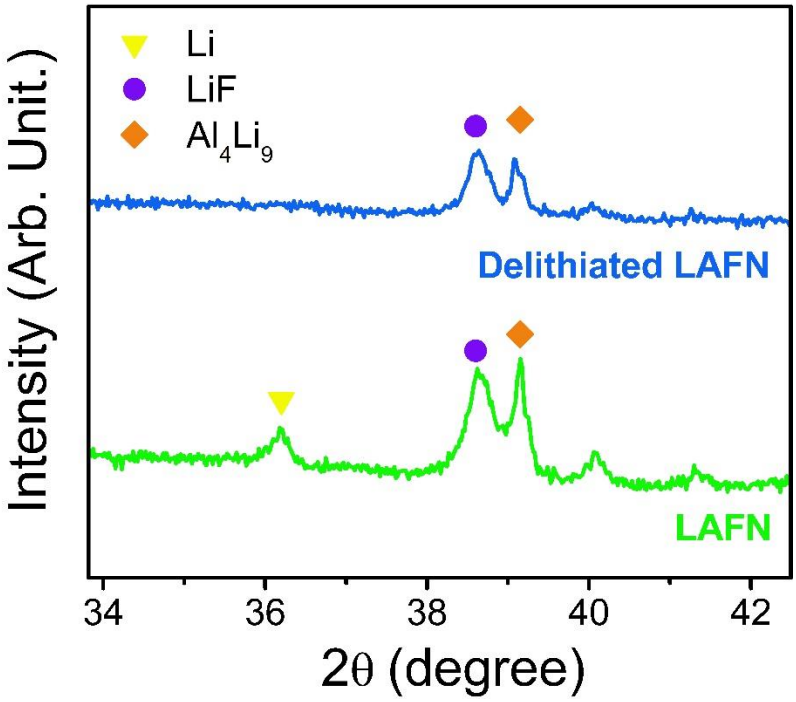

fig. S12. Enlarged XRD profile of the dotted box in Fig. 3D.

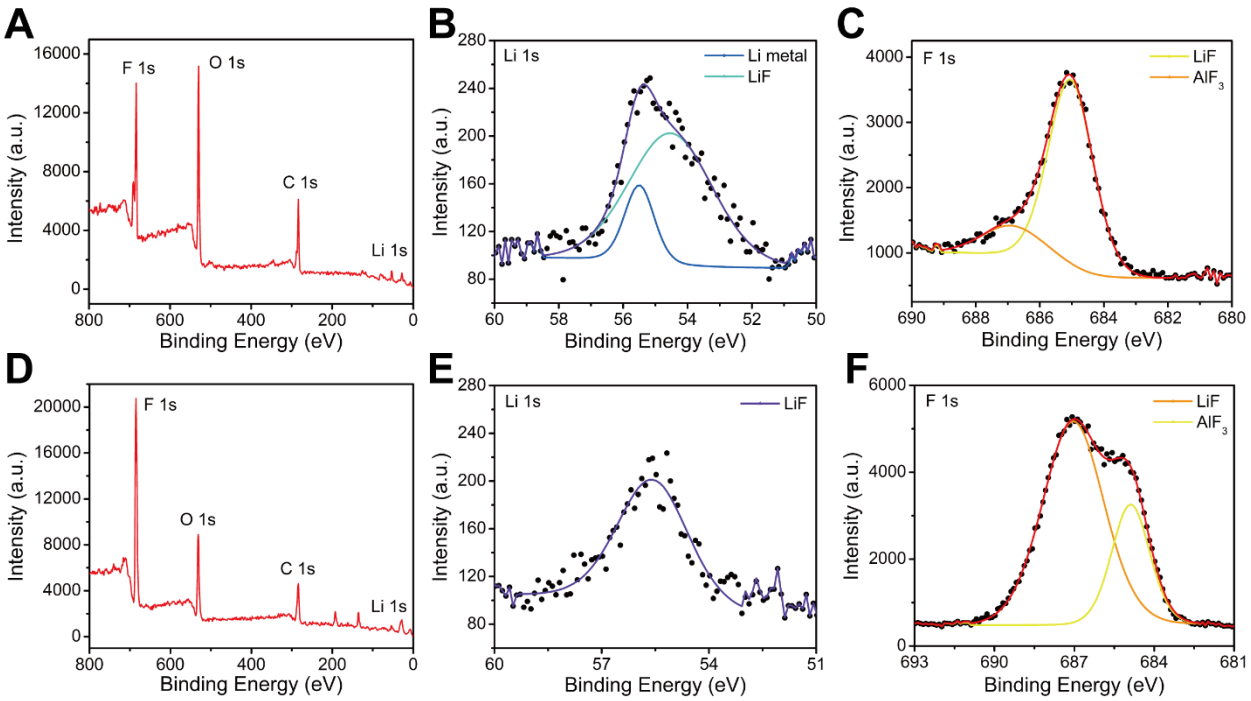

fig. S13. XPS of LAFN. (**A-C**) Survey (**A**), Li 1s (**B**), and F 1s spectra (**C**) of LAFN before stripping. (**D-F**) Survey (**D**), Li 1s (**E**) and F 1s (**F**) spectra of LAFN after excess Li metal fully stripped.

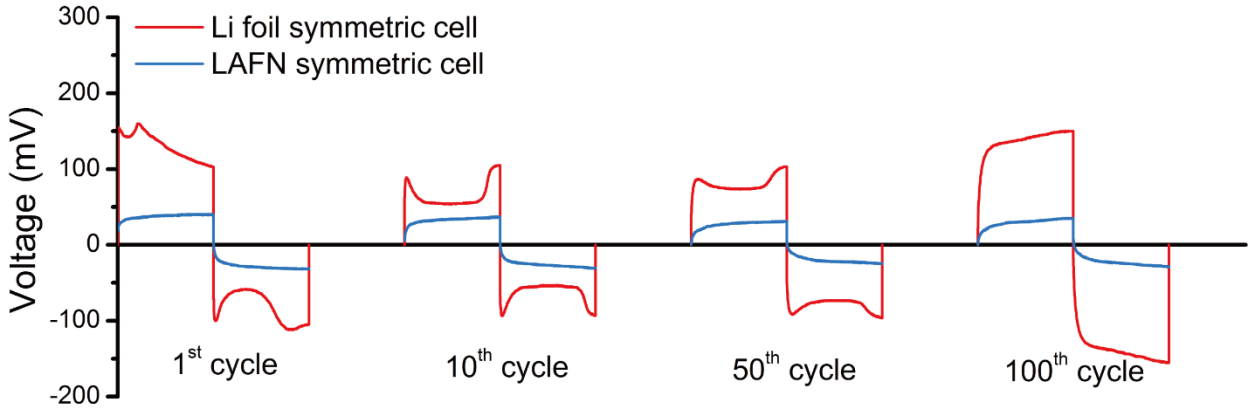

fig. S14. Voltage profile of Li foil and LAFN symmetric cell during the 1st, 10th, 50th and 100th cycles, with a current density of 1 mA cm^{-2}.

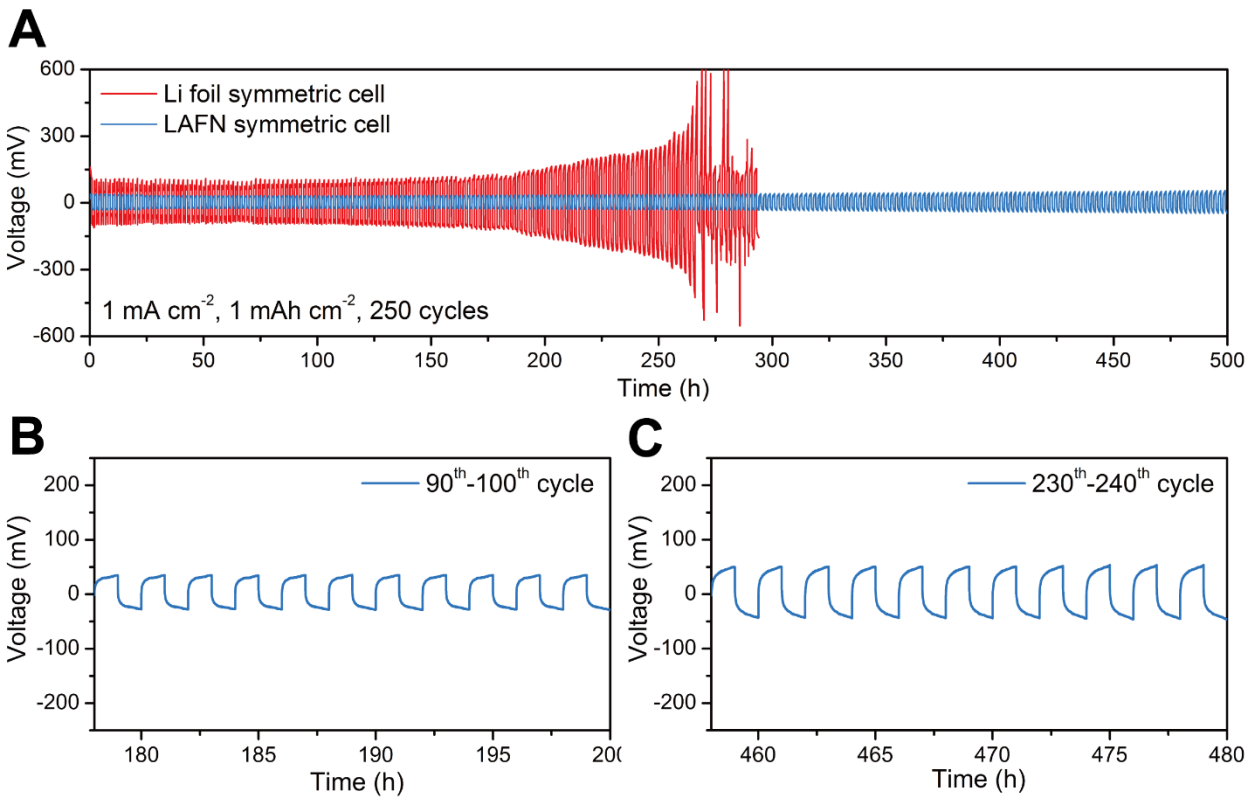

fig. S15. Long-term cycling stability of LAFN electrode. (**A**) Galvanostatic cycling of LAFN electrode symmetric cell (*blue*) and Li foil symmetric cell (*red*) in the first 500 hours (250 cycles). The current density and the areal capacity were fixed at 1 mA cm^{-2} and 1 mAh cm^{-2}, respectively. (**B**) The enlarged voltage profiles from 90th to 100th cycle. (**C**) The enlarged voltage profiles from 230th cycle to 240th cycle.

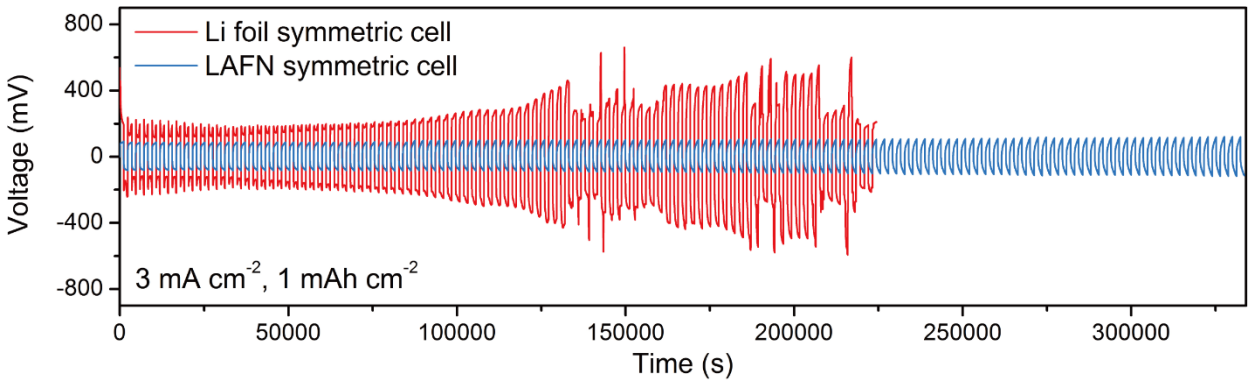

fig. S16. Symmetric cell cycling performance of LAFN under a current density of 3 mA cm^{-2}.

Symmetric cell cycling performance comparison between Li foil (*red*) and LAFN (*blue*) under 3 mA cm^{-2}. Areal capacity fixed at 1 mAh cm^{-2}.

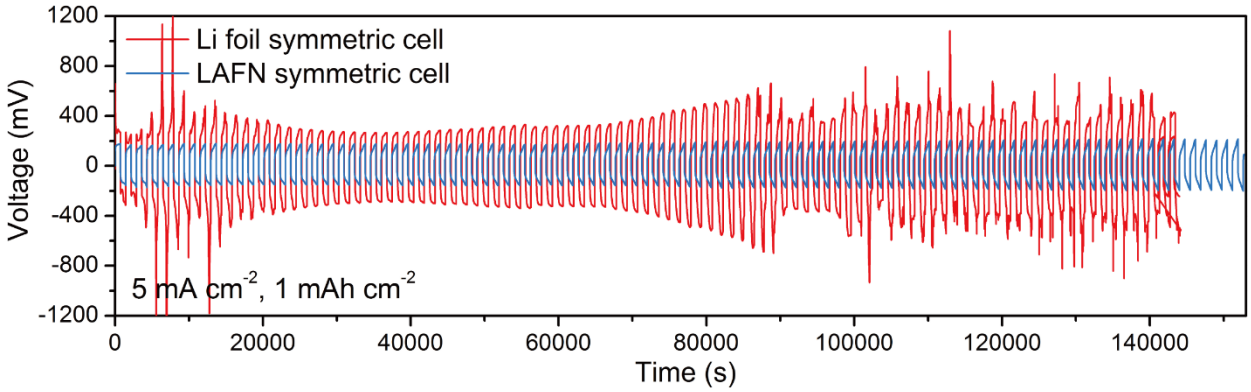

fig. S17. Symmetric cell cycling performance of LAFN under a current density of 5 mA cm^{-2}.

Symmetric cell cycling performance comparison between Li foil (*red*) and LAFN (*blue*) under 5 mA cm^{-2}. Areal capacity fixed at 1 mAh cm^{-2}.

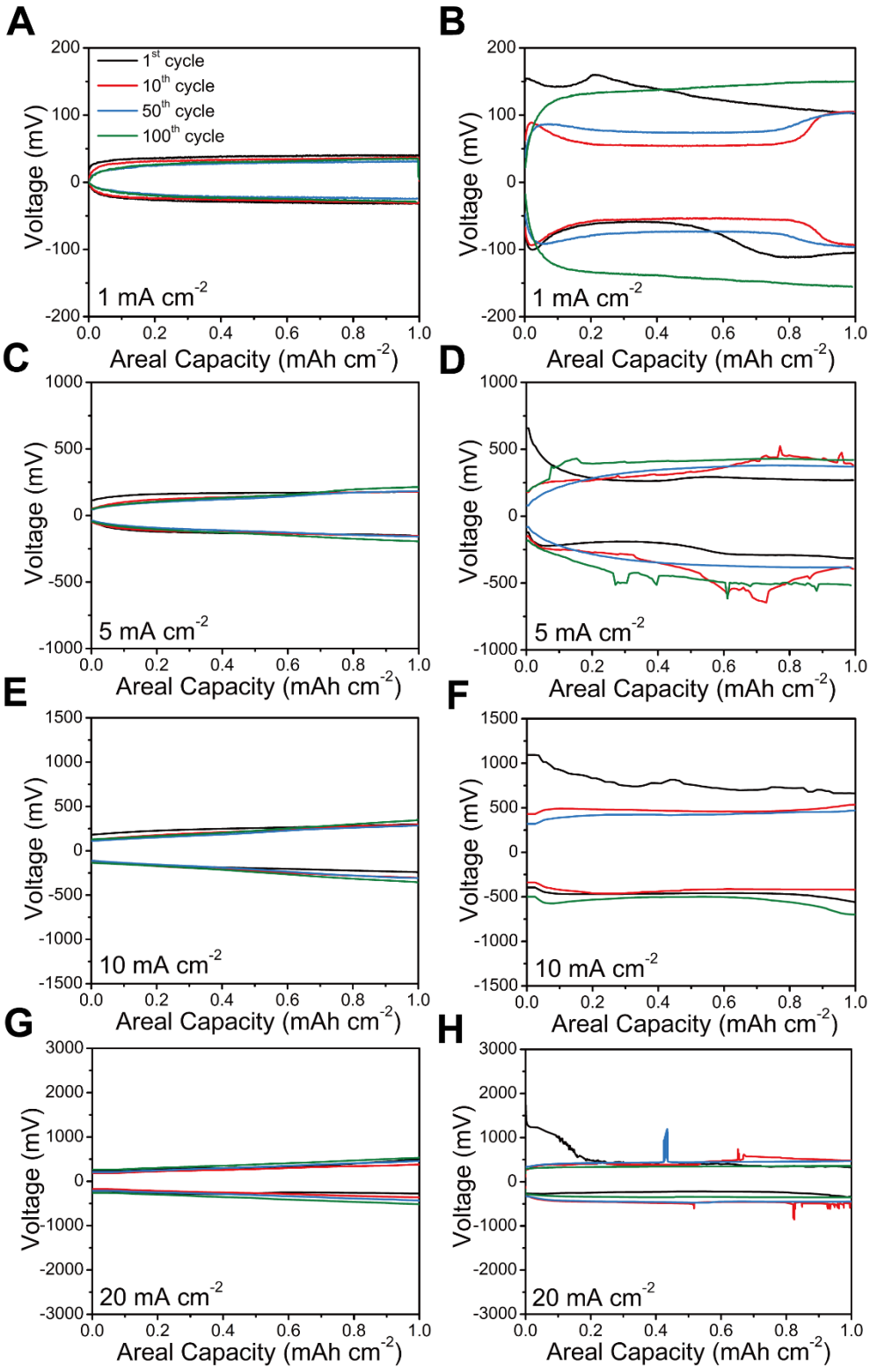

fig. S18. Voltage plateau comparison. Voltage profiles during charging and discharging processes of LAFN (**A, C, E, G**) and Li foil (**B, D, F, H**) are compared under current density of 1 mA cm^{-2}, 5 mA cm^{-2}, 10 mA cm^{-2}, 20 mA cm^{-2}, with areal capacity fixed at 1 mAh cm^{-2}.

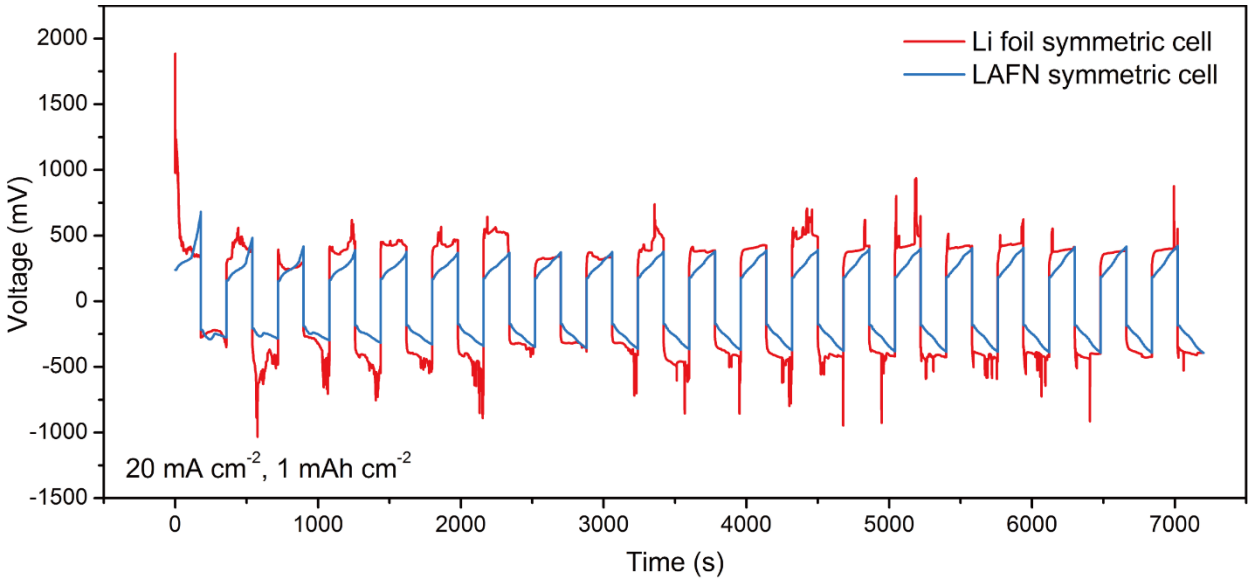

fig. S19. Symmetric cell cycling performance of LAFN under a current density of 20 mA cm^{-2}. Enlarged first 20 cycles' voltage profile of Li foil symmetric cell (*red*) and that of LAFN symmetric cell (*blue*) at a current density of 20 mA cm^{-2} and areal capacity of 1 mAh cm^{-2}.

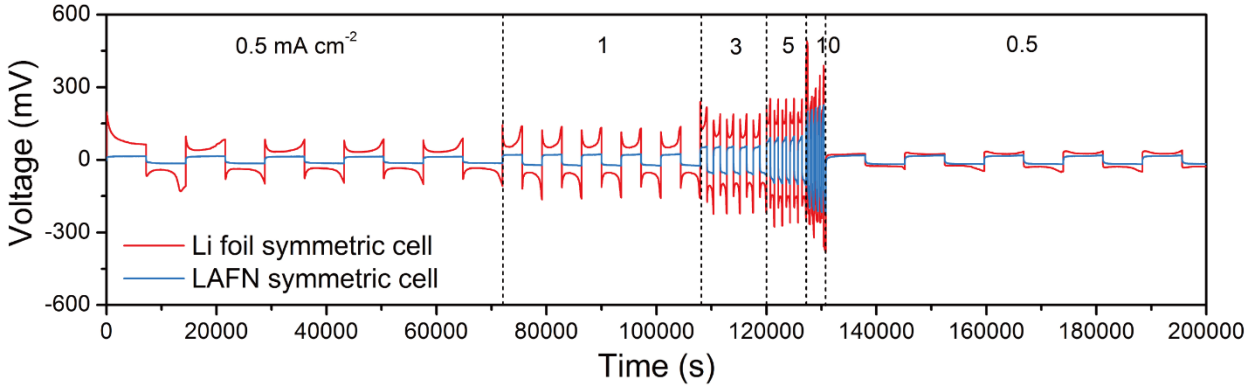

fig. S20. Symmetric cell cycling performance of LAFN under metabolic current densities. Voltage profile of Li foil symmetric cell (*red*) and that of LAFN symmetric cell (*blue*) at different current densities from 0.5 mA cm^{-2} to 10 mA cm^{-2}. Areal capacity was fixed at 1 mAh cm^{-2}.

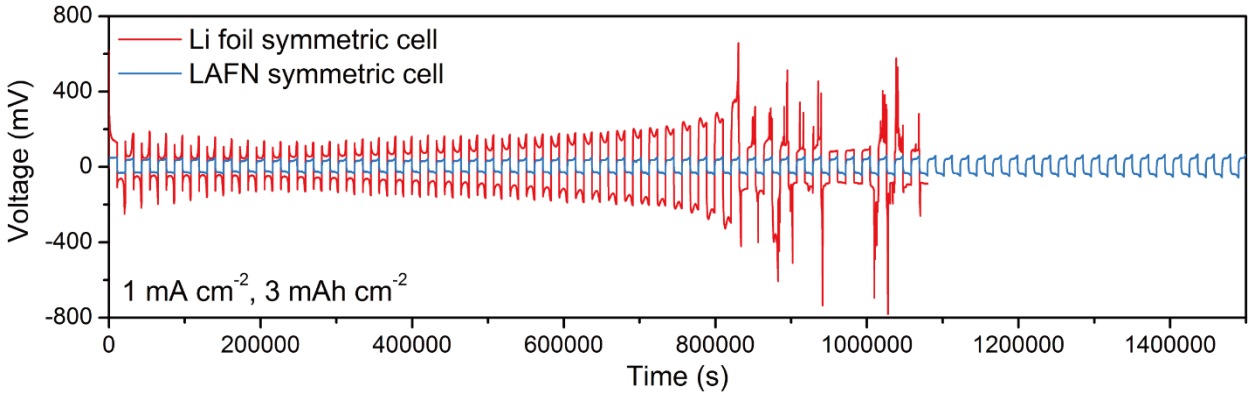

fig. S21. Symmetric cell cycling performance of LAFN under an areal capacity of 3 mA·hour cm^{-2}. Voltage profile of Li foil symmetric cell (*red*) and that of LAFN symmetric cell (*blue*) at a current density of 1 mA cm^{-2} and areal capacity of 3 mAh cm^{-2}.

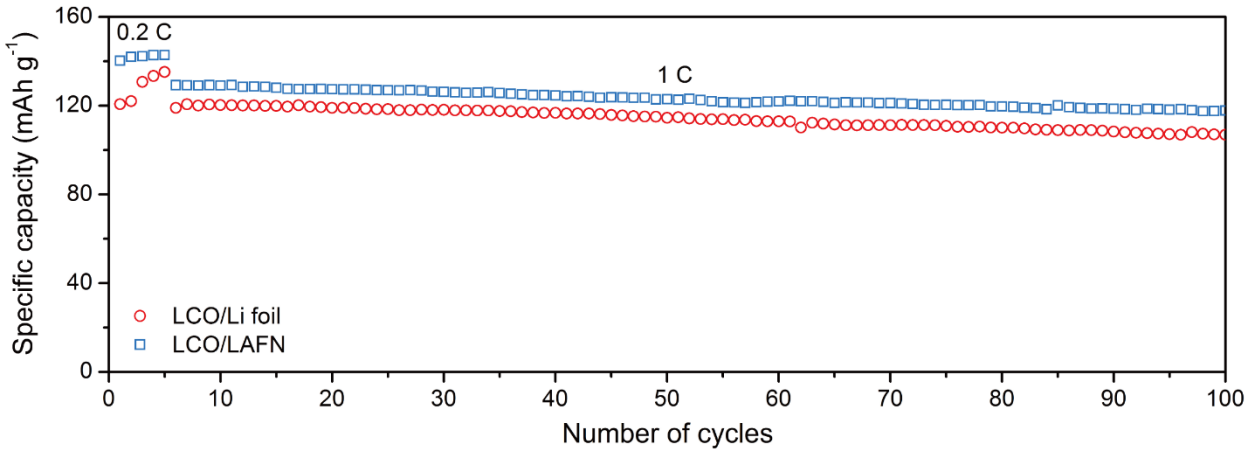

fig. S22. Electrochemical performance of LCO/LAFN cells. Long time cycling stability performance of the LCO/LAFN cells and the LCO/Li foil cells at the rate of 1 C. Activation process was performed at the initial 5 cycles with the rate of 0.2 C.

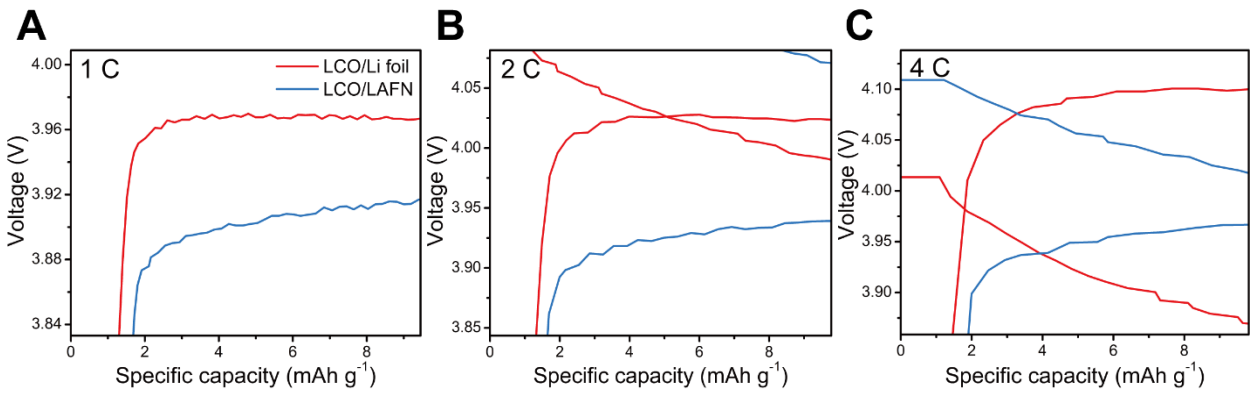

fig. S23. Enlarged voltage profile of LCO full cell batteries. (**A-C**) Enlarged voltage profile comparison of the LCO/LAFN cells and the LCO/Li foil cells at the rate of 1 C (**A**), 2 C (**B**) and 4 C (**C**), corresponding to the dotted box in **Fig. 5B-D**, respectively.

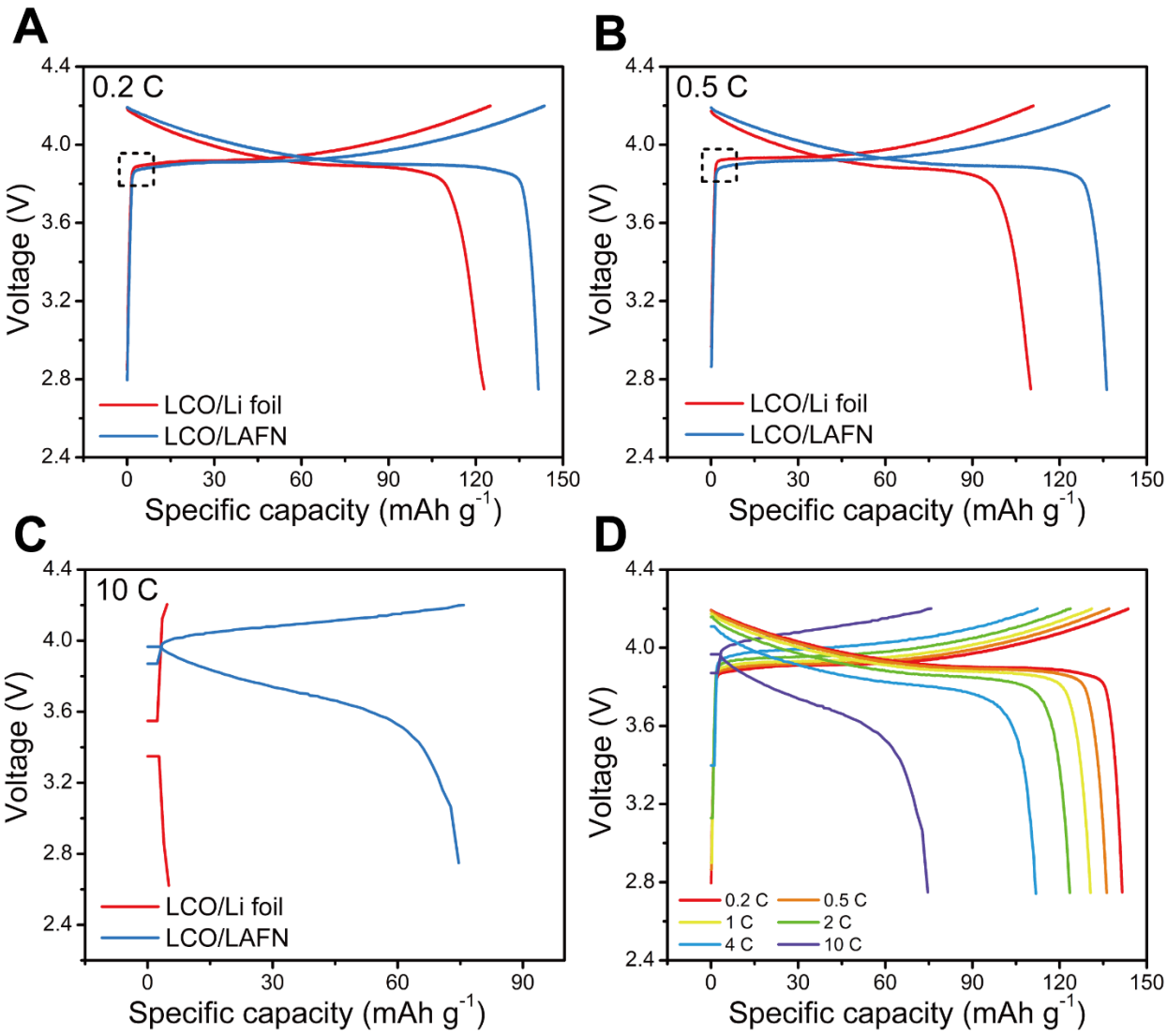

fig. S24. Electrochemical performance of LCO/LAFN cells. (**A-C**) Voltage profile comparison between LCO/LAFN cells and LCO/Li foil cells at the rate of 0.2 C (**A**), 0.5 C (**B**) and 10 C (**C**). (**D**) Voltage profiles of LCO/LAFN cells operated at various rates from 0.2 C to 10 C.

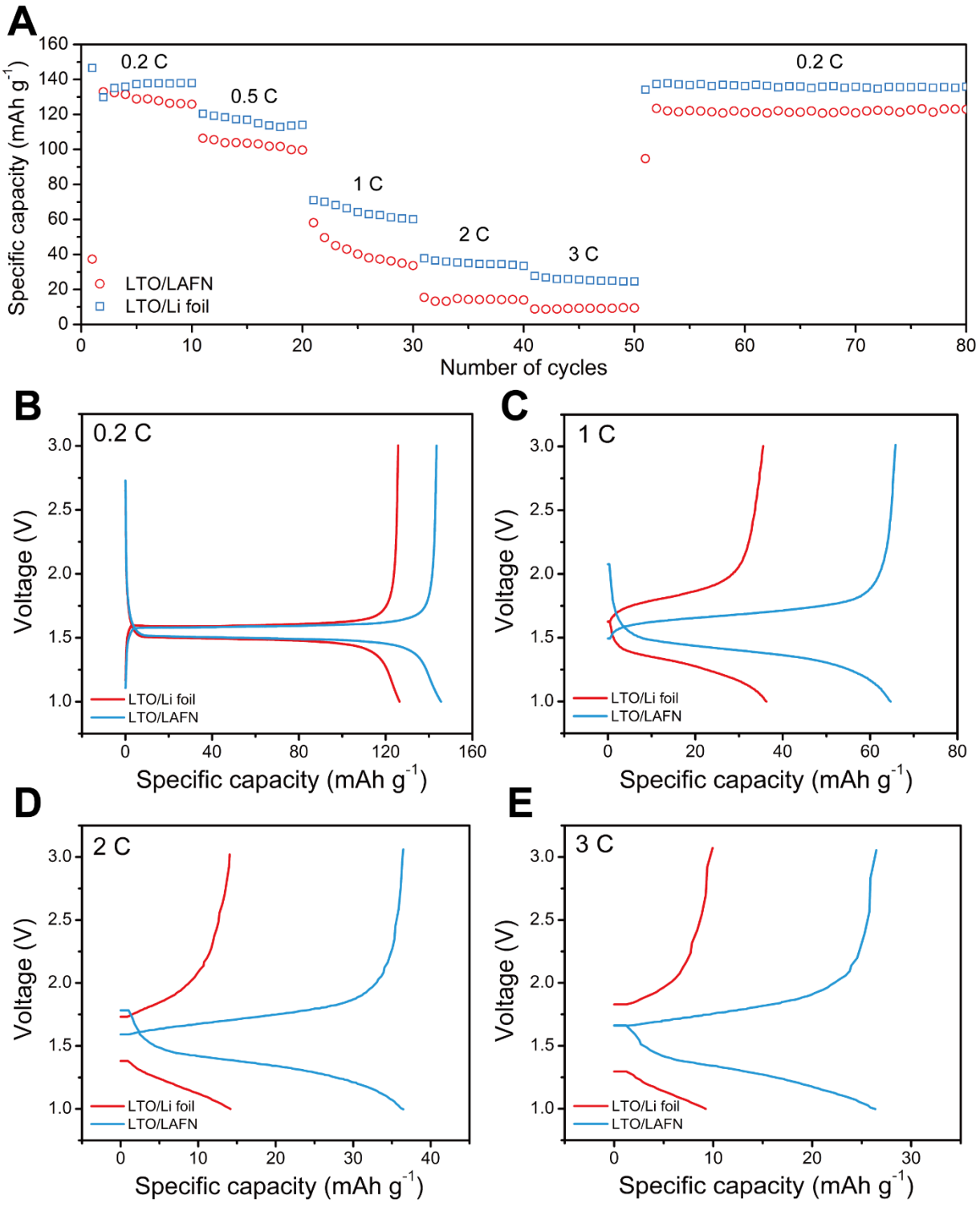

fig. S25. Electrochemical performance of LTO/LAFN cells. (**A**) Rate capability of LTO/LAFN cells and LTO/Li foil cells at various rates from 0.2 C to 3 C. (**B-E**) Voltage profile comparison between LTO/LAFN cells and LTO/Li foil cells at the rate of 0.2 C (**B**), 1 C (**C**), 2 C (**D**) and 3 C (**E**). High areal capacity of LTO (~ 3.3 mAh cm^{-2}) was used here.

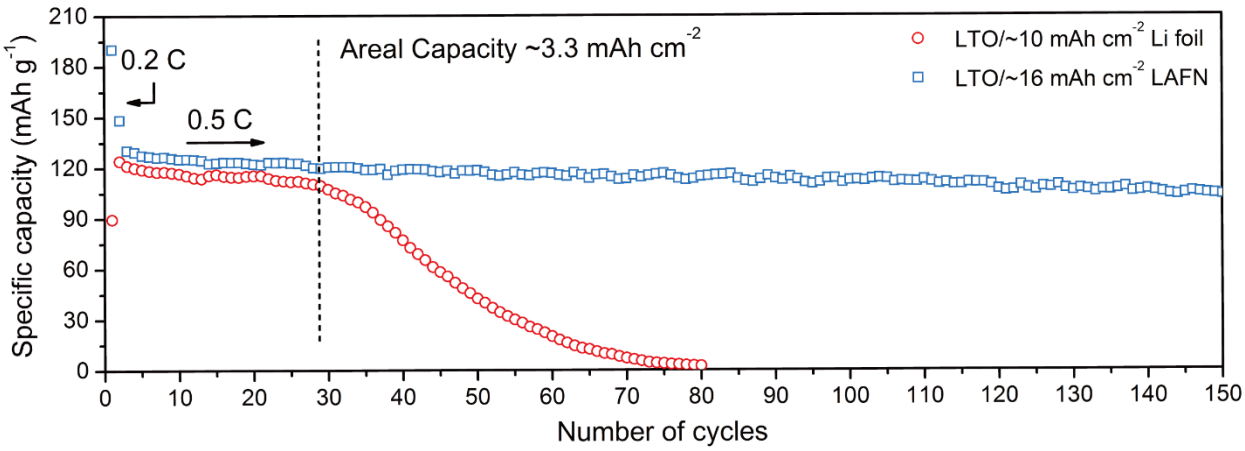

fig. S26. Electrochemical performance of LTO/LAFN cells for CE testing. Cycling stability of LTO/LAFN and LTO/Li foil cells test with limited amount of Li. High areal capacity of LTO (~ 3.3 mAh cm^{-2}) was used here. Li foil and LAFN serve as the only Li source and LTO has a high enough Coulombic efficiency. So the loss of Li can be mostly attributed to the anode (Li foil or LAFN). The point when specific capacity begins to decrease indicate the number of cycles used to consume excess Li in the anodes.